

Illuminator optimization for projection printing

E. Barouch, S. L. Knodle, S. A. Orszag, M. Yeung

Dept. of Manufacturing Engineering, Boston University, Boston MA

ABSTRACT

In this paper we report a new algorithm designed to enable printability and enhanced defocus budget at half and sub-half wavelength feature sizes. An integral part of this algorithm is the optimization of aerial image contrast, performed in stages, for an algorithmically determined set of contrast cost functions. The optimization is performed on the geometric shape of the condenser filter, herein referred to as the illuminator. Combining (1) illuminator optimization, (2) reticle proximity correction, and (3) attenuated phase shift masks (APSM) allows one to perform corrections to aggressive SRAM mask designs with feature sizes as small as 140 nm, when employing 248 nm illumination, as well as 125 nm feature sizes of lines and spaces. We also present optimizations for 80 nm lines, with 120 nm spaces using 193 nm illumination.

Keywords: half-wavelength imaging

1. INTRODUCTION

The search for improved imaging¹ has led the lithographic community to develop optical proximity correction(OPC), phase shift mask technology (PSM), off-axis illumination, condenser and exit pupil filters as well as several methods of multi-level illumination like FLEX and others. Each of these methods can improve the imaging and projection printing of microcircuit designs, but due to their non-linear nature, it is not easy to *a priori* predict when they compete against each other with degraded results. In other words, a potentially improved methodology can actually reduce printability if improperly placed. In this paper, a new algorithm is introduced addressing the non-linearity issue as applied to projection printing. In particular, an algorithm for optimizing aerial image (AI) contrast is reported, and several applications are given.

In most optimization schemes applied to realistic systems, one encounters several conceptual difficulties. Perhaps the most severe ones are the identification and interpretation of the "cost functions" and the physical "constraints". This is particularly true here, especially the selection of cost functions. In principle it looks very easy: one wants maximum contrast, maximum resolution and uniform aerial image structure throughout the entire mask design. But, unfortunately, it is unrealistic and computationally a formidable task. In other words a compromise selection process must take place to afford realistic results in reasonable time. To this end the "simplest" cost function appears to be the average slope of the AI. This slope is in fact the normal derivative which is the absolute value of the gradient on the printable contour. However, it is an impractical cost function, since during optimization it tends to degrade the worst part of the design in favor of the average, which can lead to poor printability in some domains. These domains are usually where most difficulties take place during the lithographic process, dictating the need of a cost function to concentrate initially on the features of poorest printability.

The process of optimization based on worst printable domain, is clearly design dependent. As such the optimization scheme employed must be robust enough as to account for design variability with equal or near-equal improvement capabilities. So an initial quadrapole illuminator must be chosen based on general principles associated with the actual physics of the exposure process. After some consideration, it was decided to chose the three-beam illuminator as discussed by K. Kamon². Essentially the shape is a "flared-crossed circle," meaning a circular illuminator with a removed cross, whose arms are flared outwards. This shape has been determined to closely approximate the fly's eye nature of the actual physical illuminator.

The initial optimization scheme employed is a modified conjugate-gradient with the Kamon illuminator as initial condition and worst printable slope as the initial cost function. The improvement on the minimum contrast is obtained with a systematic march, depending on the various derivatives in "illuminator space". These derivatives as well as the cost functions are obtained using our aerial image simulator FAIM. The choice of FAIM is based on its speed, accuracy, harmonic stability as well as its ability to handle a wide variety of generic illuminators, aberrations, pupil filters and non-uniform intensity throughout its illumination domain.

The next few stages of the optimization scheme employ constraints that prevents results of previous stages from worsening while the new cost function improves. The method employed improves initial contrast substantially while yielding highly improved average and maximum contrast throughout the design being optimized. Furthermore, the illuminator so obtained for one design substantially improves designs of similar nature. Last, but not least, the optimization is performed at the limiting end value of the desired defocus range, thereby improving printability throughout the entire defocus budget.

Combining algorithmically the illuminator optimization reported here with mask proximity corrections and APSM enables one to perform the necessary corrections to aggressive SRAM mask designs with feature sizes as small as 140 nm when employing 248 nm illumination, as well as 125 nm feature sizes of lines and spaces. We also present 80 nm lines with 120 nm spaces using 193 nm illumination. It is anticipated that the inclusion of E-beam proximity correction combined with optimal resist processing and plasma etching algorithms will serve as a guide to 80 nm feature size for aggressive SRAM designs and 60 nm lines for 157 nm wavelength, despite the severe non-linearity encountered in these problems.

2. METHOD

The illuminator shape is varied over a wide range of possibilities by beginning with an initial illuminator shape, usually one relatively good in the quality being optimized. In this paper, only quadrapole illuminators are considered. Annular illuminators can be represented by four symmetric arc-shaped elements.

Spline curve segments (with appropriate continuity conditions at the endpoints) are used to represent the upper right quadrant of this quadrapole illuminator as the interior of a single closed path. The control points for these spline segments are then allowed to vary freely. Complex shapes can thus be represented by a relatively small number (usually about 30) of degrees of freedom.

An appropriate cost function as described above is chosen, and a search conducted to obtain its optimum.

Each spline curve segment is subdivided into many sub-segments, and the resulting polygon-like region is subdivided into small constrained Delaunay triangles. The barycenters of these triangles, each weighted by the triangle's area, give a collection of illuminator points that are optically independent, providing an input for the simulator FAIM. The contrast cost function is then computed for the resulting aerial image intensity.

The gradient of the cost function in illuminator space is estimated by varying the spline curve's position slightly in each possible direction. It is then employed in a conjugate gradient scheme to obtain the cost function's optimal value. The specifics of the cost function, the constraints on the illuminator shape, as well as the optimization algorithm used, can then be changed, and the search may be continued as needed.

3. EXAMPLES

Lord Rayleigh's classical resolution formula suggests that a one-to-one correspondence exists between the wavelength of the imaging light and the minimum feature size resolved by it. However, with increasing numerical aperture and various optical enhancement techniques, this prediction can be improved. In this section, it is demonstrated how a combination of optical enhancement methodologies can yield half-wavelength as well as sub-half-wavelength feature sizes.

Four examples of illuminator optimization are given. Each figure represents an initial illuminator and the result of its corresponding optimization. In Fig. 1 we display the Kamon quadrapole illuminator optimized for an aggressive SRAM design, using 248 nm wavelength with 250 nm feature size. It is interesting to note that optimizing the Kamon illuminator produces a shape that is reminiscent of octagonal shapes. This observation prevails throughout a large class of optimizations performed, with designs including horizontal, vertical, and diagonal lines. It appears that the left-right and up-down symmetry provided by a quadrapole illuminator is enhanced to accommodate illuminator symmetry around the 45-degree lines as well. However, that symmetry can be distorted when a design contains a domain with sufficiently poor resolution and contrast. In Fig. 2, the result obtained from Fig. 1 is employed as initial condition of the illuminator optimization procedure using 248 nm wavelength on the SRAM design shrunk to 180 nm feature size, with a nine percent attenuated phase shift mask (APSM).

As one can see, the kidney-like illuminator changes its appearance somewhat, but in principle, retains its general shape. The design was further shrunk to 160 nm feature size, and the illuminator optimization procedure repeated,

with the result displayed in Fig. 2 employed as the initial condition. The illuminator hardly changes its shape and is shown as the solid line of both Fig. 3 and 4. When the design was further shrunk to 140 nm feature size, resolution was badly degraded using the phase-shift mask alone, resulting in significant distortion of the illuminator, as can be seen in Fig. 3. A mask correction optimization was introduced, and the illuminator was optimized a second time on this phase-shifted, OPC corrected mask. The illuminator hardly changed its shape, as can be seen in Fig. 4.

In Fig. 5 one can see the original SRAM mask design shrunk to 140 nm feature size displayed on a 50 nm grid. The result of the mask correction procedure is displayed in Fig. 6. The results of the aerial image computation are displayed in Fig. 7 and 8. In Fig. 7, the aerial image obtained from the mask displayed in Fig. 6 is embedded within the mask displayed in Fig. 5. In particular, the threshold contour obtained from the phase-shifted mask with the optimized illuminator gives very good simulated printability of this aggressive SRAM design.

In Fig. 8, the entire aerial image with its corresponding threshold contour is displayed. As one can see, the contrast associated with this imaging is very good, the minimum normal derivative of the aerial image improves from 0.92 to 1.73. That is, the minimum slope has improved from under 45 degrees to over 60 degrees. In conclusion, the combination of OPC, PSM, and illuminator optimization affords printability of an aggressive design at 140 nm feature size with 248 nm wavelength illumination.

Figures 9 - 13 show a defocus study of lines and spaces of 125 nm feature size with 185 nm spacing, again employing a combination of nine percent attenuation phase shift optimized mask design, and the optimized illuminator displayed in Fig. 4. Figures 9 - 13 display the defocus 0, 0.1, ... , 0.4, respectively. As can be seen, at 0.4 micron defocus the image is badly degraded. In other words, one achieves approximately plus/minus two and one-half feature sizes depth of focus for half-wavelength feature size printability.

Last, but not least, in Fig. 14, a display of 80 nm feature size lines and spaces is presented, with 193 nm illumination, employing the illuminator displayed in Fig. 4. We believe that our new innovative technology is a breakthrough that will help to enable sub-half-wavelength lithography. Indeed, we expect to be able to achieve even better resolution with additional optimization steps.

4. DISCUSSION

The most important observations produced by this study are:

1. An image quality cost function based on improving the worst case behavior significantly improves the worst case, while making noticeable improvements of the image as a whole.
2. Optimizing to improve the worst case behavior under high defocus conditions results in an illuminator that produces usable images over a large defocus range, and improves CD control both for line-width and shortening. Furthermore, these effects apply to other masks as well.
3. Cost functions based on global mask properties tend to badly degrade the worse regions while improving the average contrast.
4. Half wavelength feature sizes are printable with proper combination of mask proximity corrections, illuminator optimization and attenuated phase shift mask. Optimizing resist thickness is expected to yield sub-half wavelength printability of aggressive designs.

ACKNOWLEDGEMENTS

The authors acknowledge partial support from DARPA and AFOSR.

REFERENCES

1. FAIM user's manual, Vector Technologies Inc.(1998).
see also R Vallishayee, S A Orszag, E Barouch, "Stepper optimization" SPIE **2726** 660 1996.
2. K. Kamon, Ph.D. thesis, Waseda University, Tokyo, Japan(1999). See also K. Kamon, T. Miyamoto, Y. Myoi, H. Nagata, and M. Tanaka, "Photolithography System Using Modified Illumination" Jpn. J. Appl. Phys. **32**(1993), pp. 239-243.

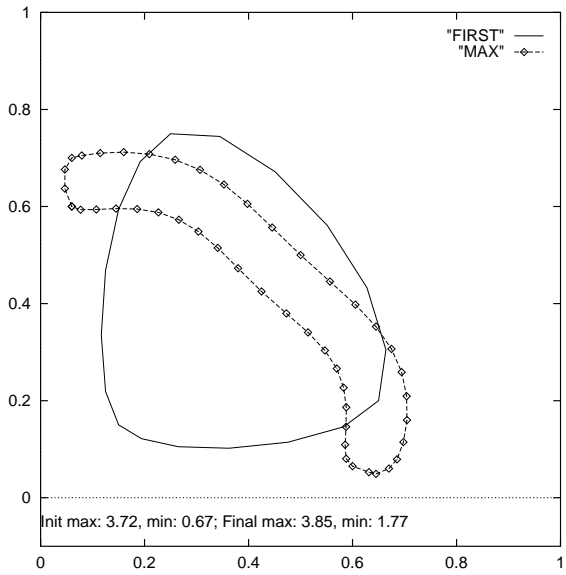


Figure 1. Kamon Three-Beam Illuminator optimized on SRAM, 250 nm Feature Size

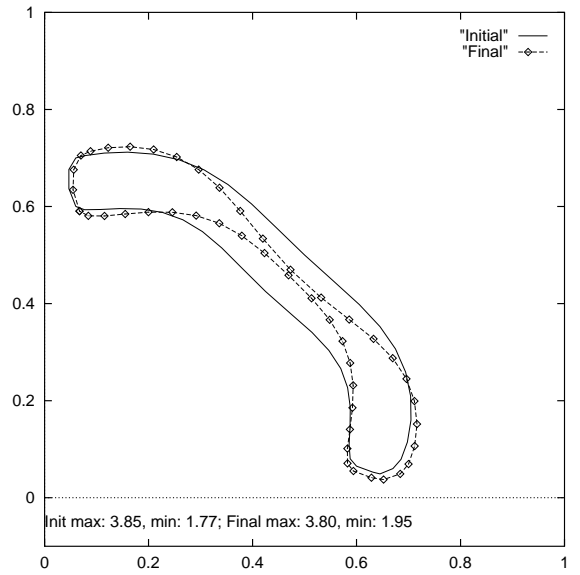


Figure 2. Optimized Illuminator, 180 nm Feature Size

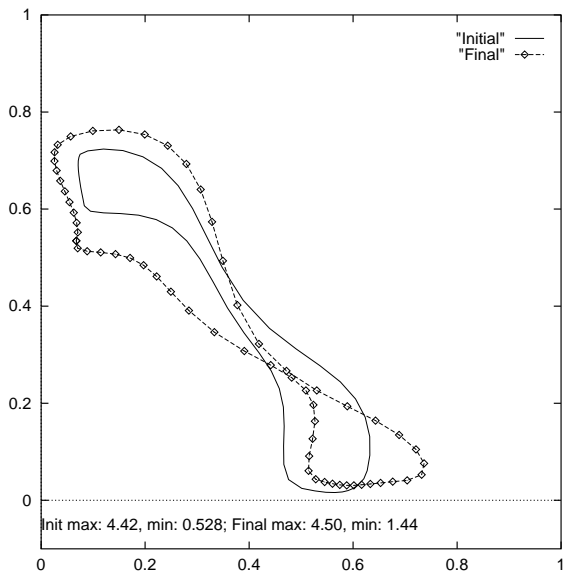


Figure 3. Illuminator Optimized on APSM Mask without OPC, 140 nm Feature Size

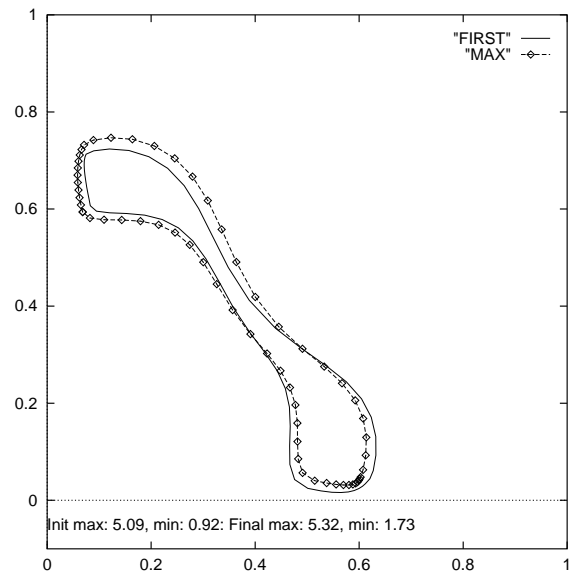


Figure 4. Illuminator Optimized on APSM Mask with OPC, 140 nm Feature Size

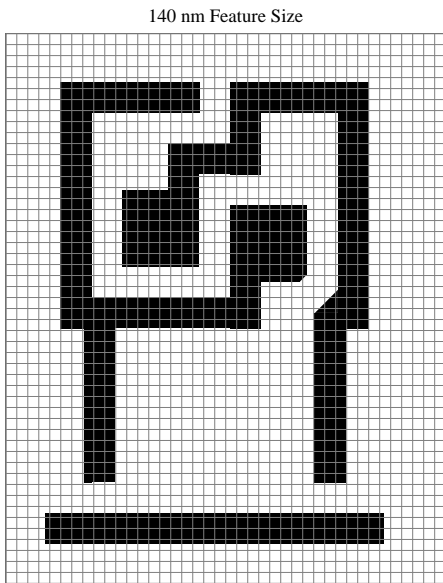


Figure 5. Original SRAM Design

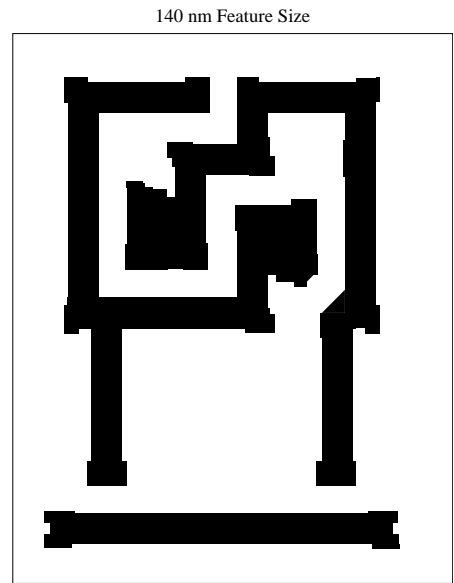


Figure 6. SRAM Design with OPC

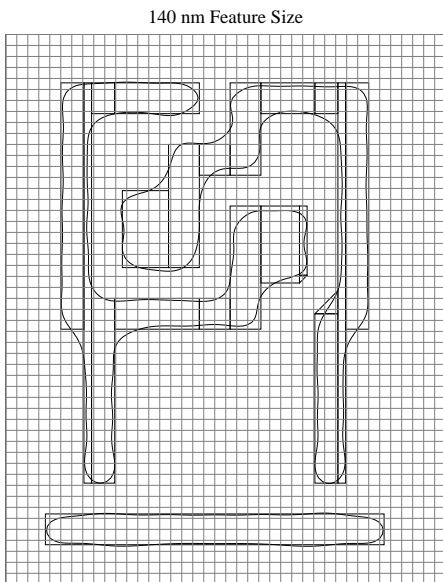


Figure 7. Intensity Contour with SRAM Mask

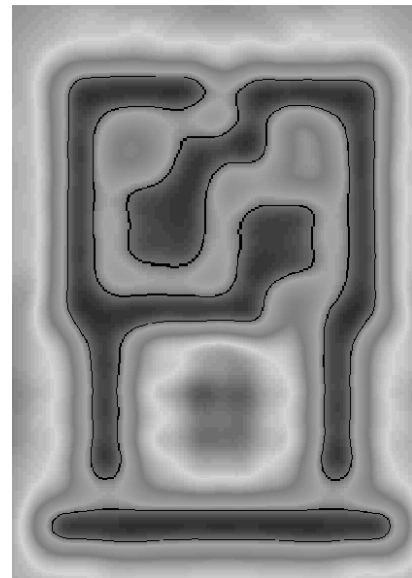


Figure 8. Shaded Aerial Image Intensity Plot

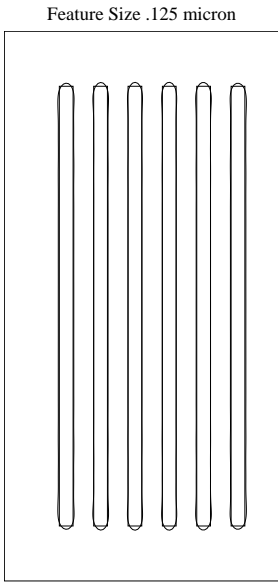


Figure 9. Defocus 0.0 micron

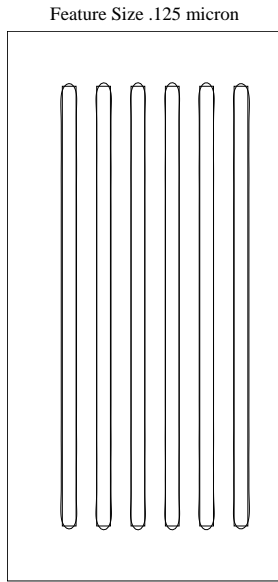


Figure 10. Defocus 0.1 micron

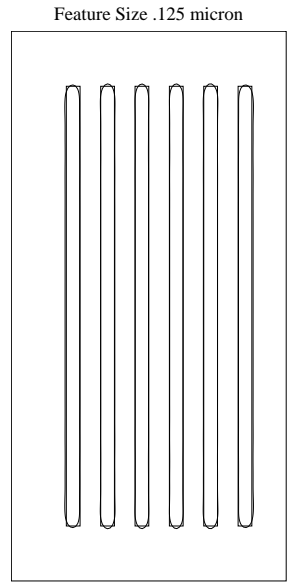


Figure 11. Defocus 0.2 micron

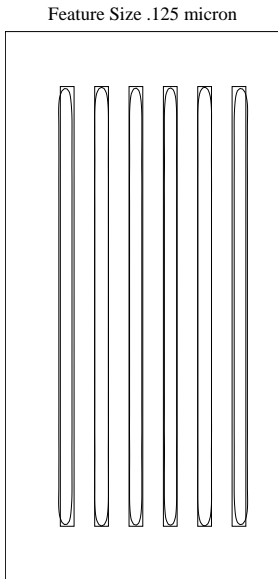


Figure 12. Defocus 0.3 micron

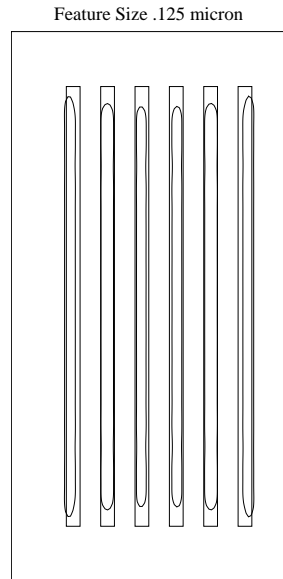


Figure 13. Defocus 0.4 micron

80 nm Feature Size

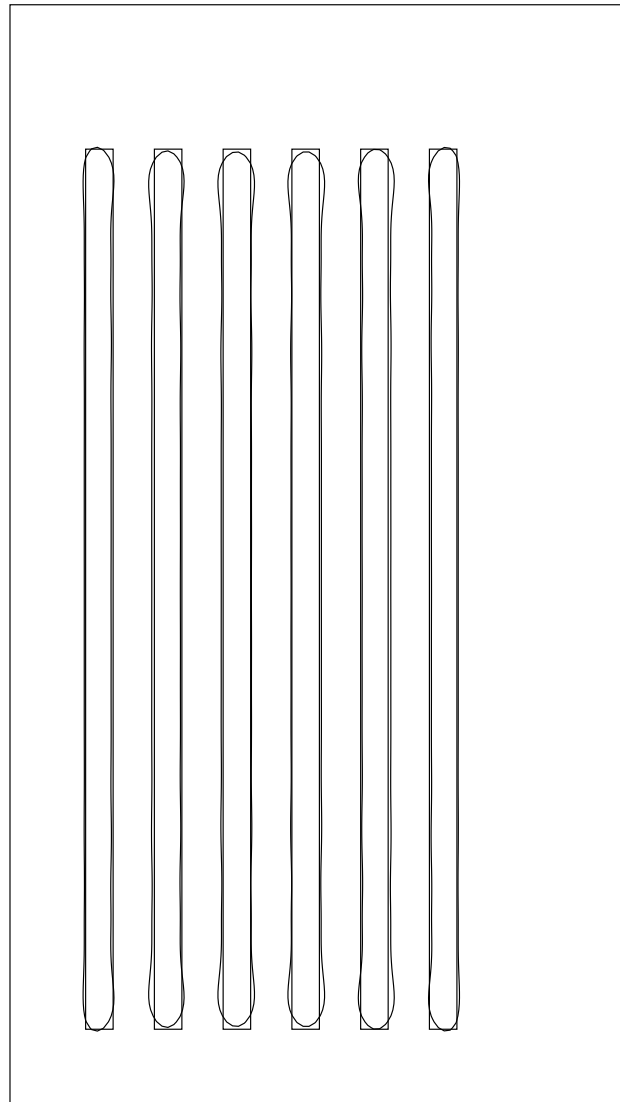


Figure 14. Feature Size 80 nm, Wavelength 193 nm